

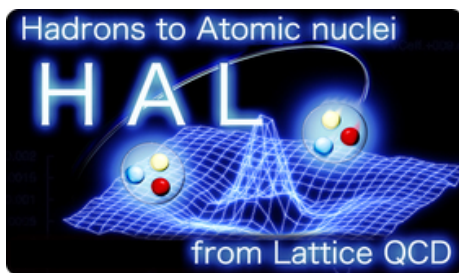
Search for possible bound T_{cc} and T_{cs} on the lattice

Yoichi Ikeda*

Theoretical Research Division, Nishina Center, RIKEN, Saitama 351-0198, Japan

E-mail: yiked@riken.jp

for HAL QCD Collaboration



Possible bound states of charmed tetraquarks $T_{cc} = (cc\bar{u}\bar{d})$ and $T_{cs} = (cs\bar{u}\bar{d})$ are studied through the s-wave meson-meson interactions, D - D , \bar{K} - D , D - D^* and \bar{K} - D^* , in (2+1)-flavor full QCD simulations with the pion mass $m_\pi \simeq 410, 570$ and 700 MeV. To treat the charm-quark dynamics properly, the relativistic heavy quark action is employed. Applying the HAL QCD method to the meson-meson systems, we extract the s-wave potentials between two mesons in lattice QCD simulations, from which the meson-meson scattering phase shifts are also calculated. The phase shifts in the isospin triplet ($I=1$) channels indicate repulsive interactions, while those in the isospin singlet ($I=0$) channels suggest attraction, growing as m_π decreases. This is particularly prominent in the $T_{cc}(J^P = 1^+, I=0)$ channel, though neither bound state nor resonance are found in the range $m_\pi = 410 - 700$ MeV.

31st International Symposium on Lattice Field Theory - LATTICE 2013

July 29 - August 3, 2013

Mainz, Germany

*Speaker.

1. Introduction

One of the long standing challenges in hadron physics is to establish and classify genuine multi-quark states other than ordinary baryons (3 quark states) and mesons (quark-antiquark states) [1]. In particular, one can expect the candidates of multi-quark configurations for charmed tetraquarks (such as T_{cc} ($cc\bar{u}\bar{d}$), T_{cs} ($cs\bar{u}\bar{d}$)) and bottomed tetraquarks (such as T_{bb} , T_{bc} , T_{bs}) [2, 3, 4, 5], since, in these channels, the so-called ‘‘good’’ diquark, $\bar{u}\bar{d}$ in the color $\mathbf{3}$, spin-singlet ($S=0$), and isospin-singlet ($I=0$) channel, due to the large attraction between \bar{u} and \bar{d} generated through a gluon exchange can be formed [6].

However, predictions for the binding energies of charmed tetraquarks widely spread, ranging from negative values (resonance) to 100 MeV (deeply bound) with respect to the two-meson thresholds, depending on the details of the dynamical models [7, 8, 9, 10], and lattice QCD (LQCD) in heavy quark limit [11, 12]. Therefore, a quantitative prediction for charmed tetraquarks requires a careful study in full LQCD with a finite charm-quark mass ¹.

In this study, we search for the charmed tetraquarks for both iso-singlet and iso-triplet T_{cc} ($J^P = 0^+, 1^+$) and T_{cs} ($J^P = 0^+, 1^+$) whose lowest meson-meson thresholds are D - D , D - D^* , \bar{K} - D and \bar{K} - D^* , respectively. By applying the HAL QCD method to extract hadronic interactions [15, 16, 17, 18, 19, 20, 21, 22, 23, 24] to charmed meson-meson systems, which was recently shown to be quite accurate for the calculation of meson-meson scattering phase shift [25], we report our first results on the potentials in the s-wave D - D ($I = 1$), D - D^* ($I = 0, 1$), \bar{K} - D ($I = 0, 1$) and \bar{K} - D^* ($I = 0, 1$) channels in (2+1)-flavor LQCD simulation. We also employ the relativistic heavy quark action [26] to treat the dynamics of the charm quarks. Then the meson-meson scattering phase shifts are derived from the corresponding potentials calculated on the lattice by the HAL QCD method.

This paper is organized as follows. In Sec. 2, we present the HAL QCD method to extract the potential between two mesons and then show the numerical setup of our lattice QCD simulations. In Sec. 3, we show our numerical results for the potentials, scattering phase shifts and scattering lengths obtained from three different quark masses. Sec. 5 is devoted to discussions and a summary.

2. HAL QCD method and numerical setup of LQCD simulations

We start with the two-meson correlation function defined as

$$\begin{aligned} F(\vec{r}, t) &\equiv \sum_{\vec{x}} \langle 0 | \mathcal{O}_{h_1}(\vec{x} + \vec{r}, t) \mathcal{O}_{h_2}(\vec{x}, t) \overline{\mathcal{J}}_{h_1 h_2}(t = 0) | 0 \rangle \\ &= \sum_n A_n \phi_n(\vec{r}) e^{-W_n t} + \dots, \end{aligned} \quad (2.1)$$

with $A_n = \langle n | \overline{\mathcal{J}}_{h_1 h_2}(t = 0) | 0 \rangle$ and $\phi_n(\vec{r}) = \sum_{\vec{x}} \langle 0 | \mathcal{O}_{h_1}(\vec{x} + \vec{r}, t) \mathcal{O}_{h_2}(\vec{x}, t) | n \rangle$. $\overline{\mathcal{J}}_{h_1 h_2}(t = 0)$ stands for a zero momentum wall source operator at $t_{\text{src.}} = 0$ which creates a two-meson state, and $\mathcal{O}_{h_{1,2}}$ is a point-like interpolating sink operator for mesons $h_{1,2}$. $\phi_n(\vec{r})$ is an equal-time Nambu-Bethe-

¹The importance of the finite charm-quark mass to extract the c - \bar{c} potentials from lattice QCD was reported previously in [13, 14].

Salpeter (NBS) wave function for n -th eigenstate $|n\rangle$ with the relativistic energy $W_n = \sqrt{m_1^2 + \vec{k}_n^2} + \sqrt{m_2^2 + \vec{k}_n^2}$, and ellipses represent inelastic contributions.

Let us consider t sufficiently larger than t_{src} , that the contributions from elastic scattering states and possible bound states remain while those from inelastic states become negligible. Then, from the NBS wave function, we define energy-independent HAL QCD potentials below inelastic threshold [16, 18] as

$$H_0 \phi_n(\vec{r}) + \int d\vec{r}' U(\vec{r}, \vec{r}') \phi_n(\vec{r}') = E_n \phi_n(\vec{r}), \quad (2.2)$$

$$U(\vec{r}, \vec{r}') = \sum_n (E_n - H_0) \phi_n(\vec{r}) \cdot \tilde{\phi}_n^*(\vec{r}'), \quad (2.3)$$

for all elastic eigenstates n , where $H_0 = -\nabla^2/2\mu$ with $\mu = m_1 m_2 / (m_1 + m_2)$ and $E_n = \vec{k}_n^2 / 2\mu$ is a non-relativistic energy. $\tilde{\phi}_n^*(\vec{r})$ is the dual basis of the NBS wave function $\phi_n(\vec{r})$.

Since the HAL QCD potentials $U(\vec{r}, \vec{r}')$ are energy-independent by definition, a normalized correlation function $R(\vec{r}, t) = F(\vec{r}, t) e^{(m_1 + m_2)t}$ satisfies [17]

$$\left(-\frac{\partial}{\partial t} - H_0 \right) R(\vec{r}, t) \simeq \sum_n A_n (E_n - H_0) \phi_n(\vec{r}) e^{-\Delta W_n t} = \int d\vec{r}' U(\vec{r}, \vec{r}') R(\vec{r}', t), \quad (2.4)$$

where the non-relativistic approximation that $\Delta W_n \equiv W_n - m_1 - m_2 = E_n + O(k^4/m_1^3, k^4/m_2^3)$ is used. This approximation is not necessary if we allow time derivatives of higher order in Eq. (2.4), which, however, are found negligible for the systems investigated in this paper. By projecting $R(\vec{r}, t)$ onto the s-states using A_1^+ representation of the cubic group, we finally obtain the leading order s-wave potentials of the velocity expansion as

$$V_{\text{LO}}(\vec{r}) = -\frac{(\partial/\partial t)R(\vec{r}, t)}{R(\vec{r}, t)} - \frac{H_0 R(\vec{r}, t)}{R(\vec{r}, t)}. \quad (2.5)$$

To extract the s-wave meson-meson potentials in Eq. (2.5) from LQCD simulation, we employ (2+1)-flavor full QCD gauge configurations generated by the PACS-CS collaboration [27, 28] on a $32^3 \times 64$ lattice with the renormalization group improved gauge action at $\beta = 1.90$ and the non-perturbative $O(a)$ -improved Wilson quark action ($C_{\text{SW}} = 1.715$) at $(\kappa_{ud}, \kappa_s) = (0.13754, 0.13640)$, $(0.13727, 0.13640)$, and $(0.13700, 0.13640)$. These parameters correspond to the lattice cutoff $a^{-1} = 2176$ MeV (lattice spacing $a = 0.0907(13)$ fm leading to the spatial lattice volume $L^3 \simeq (2.9\text{fm})^3$).

As for the charm quark, we employ a relativistic heavy quark (RHQ) action proposed in Ref. [26], which is designed to remove the leading and next-to-leading order cutoff errors associated with heavy quark mass, $\mathcal{O}((m_Q a)^n)$ and $\mathcal{O}((m_Q a)^n (a\Lambda_{\text{QCD}}))$, respectively. In our simulations, we take the same parameters as in Ref. [29]. The obtained charmed meson masses from the simulation are listed in Table 1. We have checked that the dispersion relation of the 1S charmonium states at our heaviest pion mass, $m_\pi \sim 700\text{MeV}$, gives a reasonable value of the effective speed of light, $c_{\text{eff}} = 0.987(2)$.

3. Meson-meson potentials and scattering observables

In Fig. 1, we show the results of the s-wave meson-meson potentials in the following channels related to T_{cc} and T_{cs} with $J^P = 0^+, 1^+$: D - D ($J^P = 0^+, I = 1$), \bar{K} - D ($J^P = 0^+, I = 0, 1$), D - D^*

(κ_{ud}, κ_s)	(0.13754, 0.13640)	(0.13727, 0.13640)	(0.13700, 0.13640)
m_π (MeV)	411(2)	572(2)	699(1)
m_K (MeV)	635(2)	714(1)	787(1)
m_D (MeV)	1912(1)	1946(1)	1999(1)
m_{D^*} (MeV)	2059(8)	2099(6)	2159(4)

Table 1: Meson masses obtained in this study in MeV unit.

($J^P = 1^+, I = 0, 1$), and $\bar{K}-D^*$ ($J^P = 1^+, I = 0, 1$). We find that all the potentials in the $I = 1$ channels are entirely repulsive (Fig 1(left)). This observation is consistent with the absence of good $\bar{u}\bar{d}$ diquarks in the $I = 1$ channels. We also find the weak quark mass dependence of the potentials. Therefore, it is unlikely that the potentials in these channels turn into strong attractions to form bound states even at the physical quark mass. While in the $I = 0$ channels, we find the attractive potentials at all distances, as shown in Fig 1 (right). Such attractions are again consistent with the existence of good $\bar{u}\bar{d}$ diquarks in the $I = 0$ channel, as discussed in the Introduction.

To investigate the possible existence of bound states or resonances in the $I = 0$ channels, we fit the potentials in Fig. 1(right) with five-range-gauss analytic functions and solve the Schrödinger equation with the fitted potentials. Fig. 2 shows the resultant s-wave scattering phase shifts as a function of the meson-meson center-of-mass energy in the $I = 0$ channels $\bar{K}-D$ ($J^P = 0^+$), $D-D^*$ ($J^P = 1^+$) and $\bar{K}-D^*$ ($J^P = 1^+$). In Table 2, we give the corresponding scattering lengths. Fig. 2

m_π (MeV)	411(2)	572(2)	699(1)
$a_{\bar{K}D}$ (fm)	0.335(19)	0.308(21)	0.301(17)
a_{DD^*} (fm)	0.712(198)	0.592(192)	0.287(58)
$a_{\bar{K}D^*}$ (fm)	0.349(27)	0.335(68)	0.245(27)

Table 2: Scattering lengths in the $I = 0$ channels for the $\bar{K}-D$, $D-D^*$ and $\bar{K}-D^*$ systems.

indicates that there are no bound states or resonances in this range of pion masses, $m_\pi = 410 \sim 700$ MeV. Meanwhile, the low-energy meson-meson attraction in the $I = 0$ channel becomes stronger as the pion mass decreases, as shown in Table 2. This is particularly so for the $D-D^*$ ($J^P = 1^+, I = 0$) channel, which corresponds to $T_{cc}(J^P = 1^+, I = 0)$. Since the potentials for $D-D^*$ and $\bar{K}-D^*$ are not so much different, as seen in the left three panels of Fig. 2, a faster increase of the scattering length as a function of the pion mass in the $D-D^*$ channel than in the $\bar{K}-D$ and $\bar{K}-D^*$ channels can be attributed to the smaller kinetic energy due to double charmed $D-D^*$ system. A similar tendency has also been reported in studies of phenomenological models (see e.g. [7]).

Although we find a good evidence of a sizable attraction in the $I = 0$ channel at $m_\pi = 410 \sim 700$ MeV, the existence of a bound or resonant $T_{cc}(J^P = 1^+, I = 0)$ at the physical point remains an open question².

²If we take the same attractive potential as $D-D^*$ ($J^P = 0^+, I = 0$) at $m_\pi = 410$ MeV and calculate the $B-B^*$ ($J^P = 0^+, I = 0$) channel with the physical masses of B and B^* , we find a bound state with the binding energy 5.7(2.3) MeV.

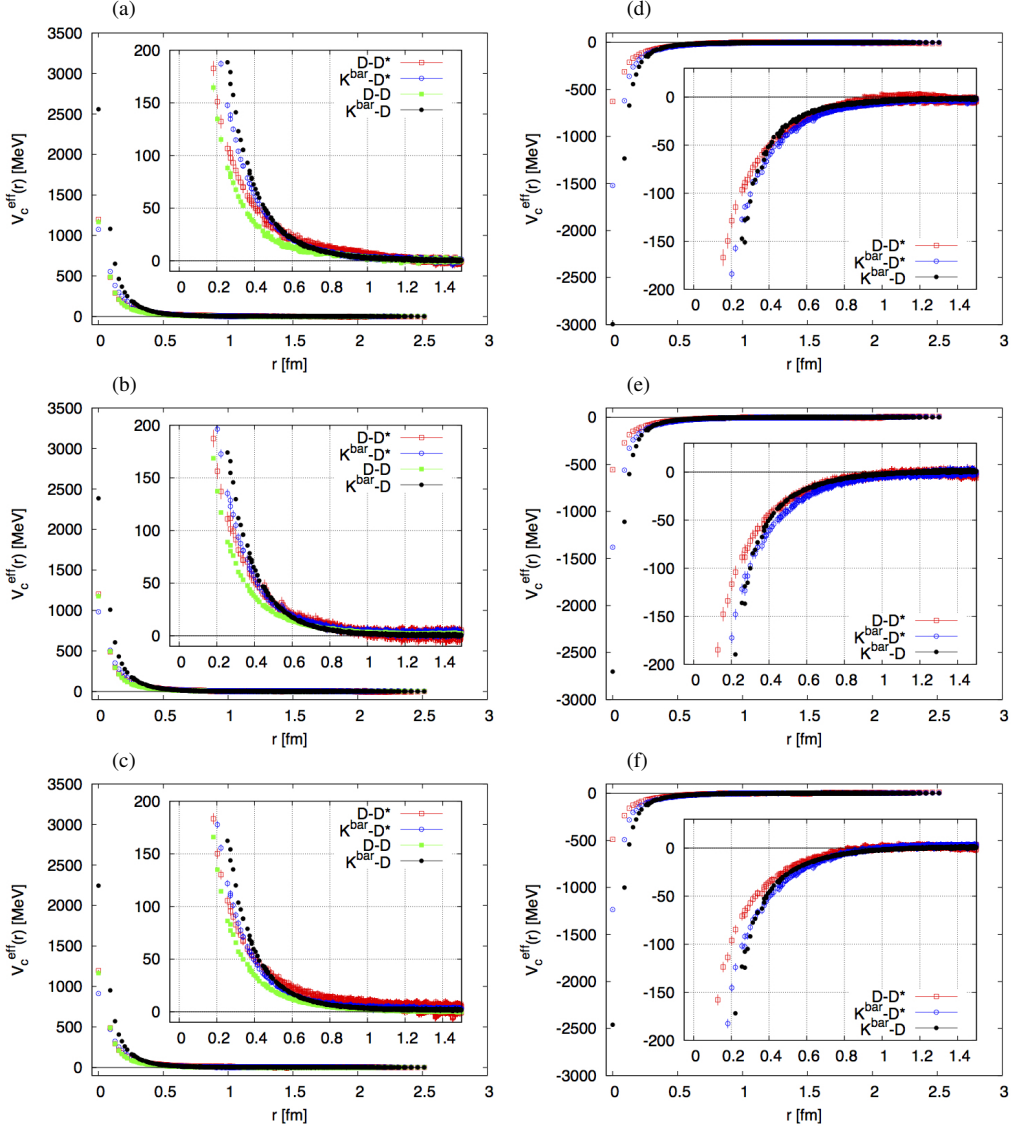


Figure 1: (color online) Left three panels for the s-wave central potentials in the iso-triplet $D-D^*$ (red square), $\bar{K}-D^*$ (blue circle), $D-D$ (green filled square) and $\bar{K}-D$ (black filled circle) channels. Right three panels for the s-wave central potentials in the iso-singlet $D-D^*$ (red square) and $\bar{K}-D^*$ (blue circle) and $\bar{K}-D$ (black filled circle) channels. (a), (b) and (c) ((d), (e) and (f)) are obtained at $m_\pi \simeq 410$ MeV, $m_\pi \simeq 570$ MeV and $m_\pi \simeq 700$ MeV, respectively.

4. Summary

We have studied the s-wave meson-meson interactions in several $I = 0$ and $I = 1$ channels ($D-D$, $\bar{K}-D$, $D-D^*$ and $\bar{K}-D^*$), using (2+1)-flavor full QCD gauge configurations generated at $m_\pi = 410 \sim 700$ MeV, in order to look for the possible existence of bound charmed tetraquark states (T_{cc} and T_{cs}). For the charm quark, we have employed the relativistic heavy-quark action to account for its proper dynamics on the lattice.

The s-wave meson-meson energy-independent potentials are extracted from Nambu-Bethe-

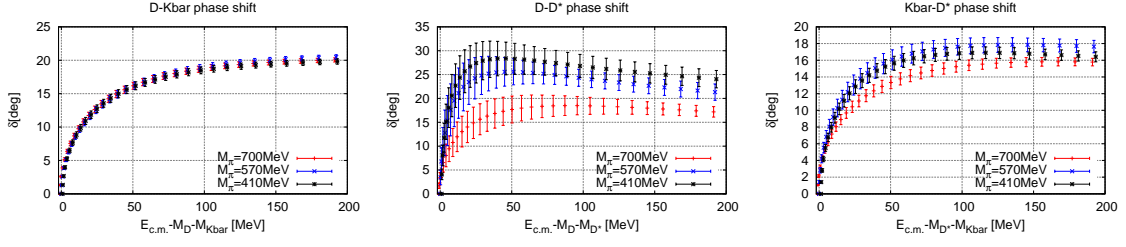


Figure 2: S-wave scattering phase shifts in the $I = 0$ $\bar{K}-D$ (left), $D-D^*$ (center) and $\bar{K}-D^*$ (right) channels.

Salpeter wave functions using the HAL QCD method. The energy-independent HAL QCD potentials are then used to calculate scattering phase shifts and scattering lengths. The s-wave meson-meson interactions in the $I = 1$ channels are found to be repulsive and insensitive to the pion mass in the region we explored, so that tetraquark bound states are unlikely to be formed even at the physical pion mass. On the other hand, the s-wave interactions in the $I = 0$ channels show attractions in the $\bar{K}-D$, $D-D^*$ and $\bar{K}-D^*$ channels, which are qualitatively consistent with the phenomenological diquark picture. The s-wave scattering phase shifts and scattering lengths in these attractive channels indicate, however, that no bound states or resonances are formed at the pion masses used in the present study, $m_\pi = 410 - 700$ MeV, though attractions become more prominent as the pion mass decreases, particularly in the $I = 0$ $D-D^*$ channel corresponding to $T_{cc}(J^P = 1^+, I = 0)$.

For a definite conclusion on the fate of T_{cc} and T_{cs} in the real world, simulations near or at the physical point are necessary. We are planning to carry out such simulations with the PACS-CS (2+1)-flavor full QCD configurations with coupled-channel schemes [30, 31].

Acknowledgment

The authors thank T. Hyodo, T. Matsuki, M. Oka, S. Takeuchi, M. Takizawa and S. Yasui for fruitful discussions, and authors and maintainer of CPS++ [32], whose modified version is used in this paper. We also thank ILDG/JLDG [33] for providing us with full QCD gauge configurations used in this study. Numerical calculations were carried out on NEC-SX9 and SX8R at Osaka University and SR16000 at YITP in Kyoto University. This project is supported in part by Grant-in-Aid for Scientific Research on Innovative Areas(No.2004:20105001, 20105003) and for Scientific Research(Nos. 25800170, 25287046, 24740146, 24540273, 23540321), and SPIRE (Strategic Program for Innovative Research).

References

- [1] R.L. Jaffe, Phys. Rev. Lett. **38** (1977) 195.
- [2] S. Zouzou, B. Silvestre-Brac, C. Gignoux and J. M. Richard, Z. Phys. C **30** (1986) 457.
- [3] H.J. Lipkin, Phys. Lett. **B 172** (1986) 242.
- [4] J. Carlson, L. Heller and J. A. Tjon, Phys. Rev. D **37** (1988) 744.
- [5] A. V. Manohar and M. B. Wise, Nucl. Phys. B **399** (1993) 17.

- [6] A. Selem and F. Wilczek, hep-ph/0602128.
- [7] S. H. Lee and S. Yasui, Eur. Phys. J. C **64** (2009) 283.
- [8] T. F. Carames, A. Valcarce and J. Vijande, Phys. Lett. B **699** (2011) 291.
- [9] S. Ohkoda, Y. Yamaguchi, S. Yasui, K. Sudoh and A. Hosaka, Phys. Rev. D **86** (2012) 034019, and references therein.
- [10] J. Vijande, A. Valcarce and J. -M. Richard, Phys. Rev. D **87** (2013) 034040 [arXiv:1301.6212 [hep-ph]].
- [11] Z. S. Brown and K. Orginos, Phys. Rev. D **86** (2012) 114506 [arXiv:1210.1953 [hep-lat]].
- [12] P. Bicudo and M. Wagner, arXiv:1209.6274 [hep-ph].
- [13] Y. Ikeda and H. Iida, Prog. Theor. Phys. **128** (2012) 941 [arXiv:1102.2097 [hep-lat]].
- [14] T. Kawanai and S. Sasaki, Phys. Rev. Lett. **107** (2011) 091601 [arXiv:1102.3246 [hep-lat]].
- [15] N. Ishii, S. Aoki and T. Hatsuda, Phys. Rev. Lett. **99** (2007) 022001.
- [16] S. Aoki, T. Hatsuda and N. Ishii, Prog. Theor. Phys. **123** (2010) 89.
- [17] N. Ishii *et al.* [HAL QCD Collaboration], Phys. Lett. B **712** (2012) 437.
- [18] S. Aoki *et al.* [HAL QCD Collaboration], PTEP **2012** (2012) 01A105.
- [19] H. Nemura, N. Ishii, S. Aoki and T. Hatsuda, Phys. Lett. **B673** (2009) 136.
- [20] T. Inoue *et al.* [HAL QCD Collaboration], Prog. Theor. Phys. **124** (2010) 591.
- [21] T. Inoue *et al.* [HAL QCD Collaboration], Phys. Rev. Lett. **106** (2011) 162002.
- [22] K. Murano, N. Ishii, S. Aoki and T. Hatsuda, Prog. Theor. Phys. **125** (2011) 1225.
- [23] T. Doi *et al.* [HAL QCD Collaboration], Prog. Theor. Phys. **127** (2012) 723 [arXiv:1106.2276 [hep-lat]].
- [24] K. Murano, N. Ishii, S. Aoki, T. Doi, T. Hatsuda, Y. Ikeda, T. Inoue and H. Nemura *et al.*, arXiv:1305.2293 [hep-lat].
- [25] T. Kurth, N. Ishii, T. Doi, S. Aoki and T. Hatsuda, arXiv:1305.4462 [hep-lat].
- [26] S. Aoki, Y. Kuramashi and S. -i. Tominaga, Prog. Theor. Phys. **109** (2003) 383.
- [27] S. Aoki *et al.* [PACS-CS Collaboration], Phys. Rev. D **79** (2009) 034503.
- [28] S. Aoki *et al.* [PACS-CS Collaboration], Phys. Rev. D **81** (2010) 074503.
- [29] Y. Namekawa *et al.* [PACS-CS Collaboration], Phys. Rev. D **84** (2011) 074505.
- [30] S. Aoki, B. Charron, T. Doi, T. Hatsuda, T. Inoue and N. Ishii, Phys. Rev. D **87** (2013) 3, 034512 [arXiv:1212.4896 [hep-lat]].
- [31] K. Sasaki [HAL QCD Collaboration], PoS LATTICE **2012** (2012) 157.
- [32] Columbia Physics System (CPS), <http://qcdoc.phys.columbia.edu/cps.html>
- [33] International Lattice Data Grid, <http://www.lqcd.org/ildg>; Japan Lattice Data Grid, <http://jldg.org>